Chemical Science

EDGE ARTICLE

View Article Online
View Journal | View Issue

Open Access Article. Published on 10 December 2013. Downloaded on 2/11/2026 1:50:36 PM.
This article is licensed under a Creative Commons Attribution 3.0 Unported Licence.

Cite this: *Chem. Sci.*, 2014, **5**, 1008

# Synthesis and properties of fully-conjugated indacenedithiophenes†

Brian S. Young, Daniel T. Chase, Jonathan L. Marshall, Chris L. Vonnegut, Lev N. Zakharov and Michael M. Haley*

Received 19th November 2013
Accepted 9th December 2013

DOI: 10.1039/c3sc53181c

www.rsc.org/chemicalscience

The synthesis and characterization of four fully-conjugated indacenedithiophenes (IDTs) are disclosed. In contrast to anthradithiophenes, regioselective synthesis of both *syn* and *anti* isomers is readily achieved. Thiophene fusion imparts increased paratropic character on the central indacene core as predicted by DFT calculations and confirmed by $^{1}$H NMR spectroscopy. IDTs exhibit red-shifted absorbance maxima with respect to their all-carbon analogues and undergo two-electron reduction and one-electron oxidation.

## Introduction

In recent years, there has been tremendous interest in highly conjugated polycyclic hydrocarbons, such as the higher acenes, because of their fascinating optical and electronic properties.[1] Although pentacene (**1**, Fig. 1) and its derivatives have been utilized in device applications such as field effect transistors, photovoltaics, and light emitting diodes, these molecules are susceptible to oxidative and photolytic degradation;[2] therefore, alternative, acene-like topologies have been explored.[3–6] One of the initial substitutes for pentacene was structurally analogous anthradithiophene (ADT, **2**), as inclusion of heterocycles allows for tuning of physical and electronic properties.[7] Thieno-fusion as part of the acene skeleton is a particularly attractive option for a number of reasons including high electron mobilities, increased stability, and ease of functionalization. In fact, hole mobilities of **2** and derivatives approach values observed for **1** yet the former exhibit improved oxidative stability.[8] As a whole, these structurally-related acene molecules and myriad derivatives behave typically as organic p-type compounds. Comparatively, there are considerably fewer organic n-type structures in the literature; thus, there is a pressing need for new molecular frameworks that can transport electrons.

Very recently, our group[9] and others[10] have begun to examine the isomers of indenofluorenes[11] (IFs, Fig. 2) as potential n-type materials due to their ability to reversibly accept two electrons. The stability and electronic properties of the IFs can be tuned by functionalization at a number of positions. Our initial studies showed that a range of electron-rich and electron-poor groups at the 2 and 8 positions of the indeno[1,2-*b*]fluorene skeleton (*e.g.*, **3a**)[9b] had only a modest effect on the electronic properties of these compounds; however, we demonstrated subsequently that functionalizing the [1,2-*b*]IFs with aryl groups at the 6 and 12 positions (**3b**)[9c] resulted in much greater variability in the redox properties of the molecules, with some displaying amphoteric behaviour. Tobe and our group reported, respectively, that [2,1-*a*] isomer **4**[10a] and previously unknown [2,1-*c*] isomer **5**[9d] also possessed excellent electrochemical properties

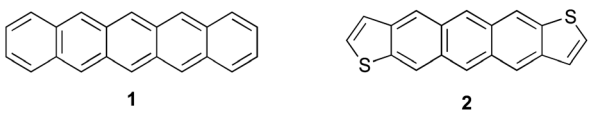


1 2

Fig. 1 Pentacene (**1**) and structural analogue anthradithiophene (ADT, **2**).

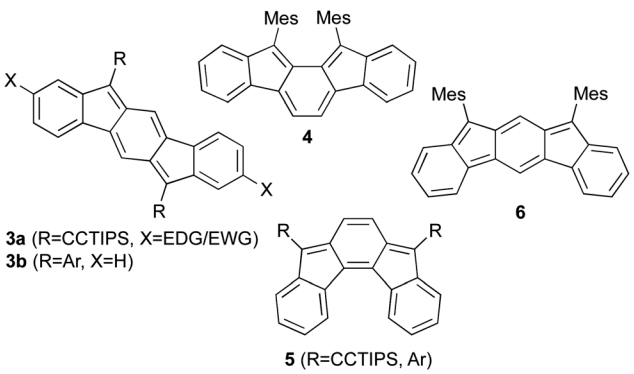


Fig. 2 Recently reported indenofluorene structures **3**–**6**.

*Department of Chemistry & Biochemistry and Materials Science Institute, University of Oregon, Eugene, OR 97403-1253, USA. E-mail: haley@uoregon.edu; Fax: +1 541-346-0487; Tel: +1 541-346-0456*

† Electronic supplementary information (ESI) available: Experimental details, spectroscopic data, computational details, and copies of $^{1}$H and $^{13}$C NMR spectra. CCDC 949864–949866, 962726. For ESI and crystallographic data in CIF or other electronic format see DOI: 10.1039/c3sc53181c



This journal is © The Royal Society of Chemistry 2014

Open Access Article. Published on 10 December 2013. Downloaded on 2/11/2026 1:50:36 PM.
This article is licensed under a Creative Commons Attribution 3.0 Unported Licence.

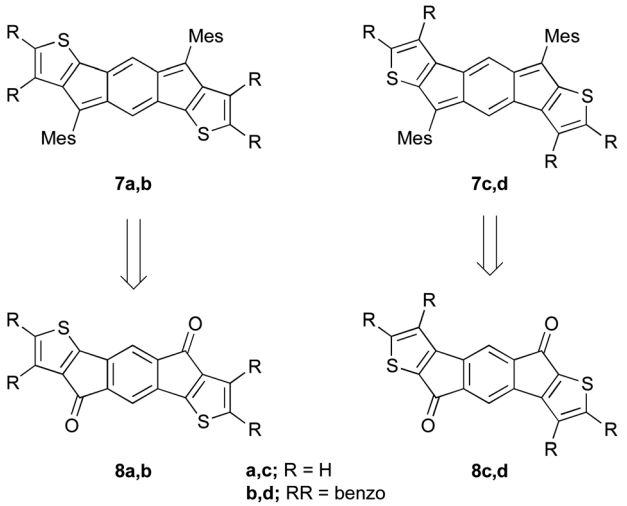


Fig. 3 Targeted structures of IDTs **7a,c** and IDBTs **7b,d** synthesized from the corresponding diones **8a–d**.

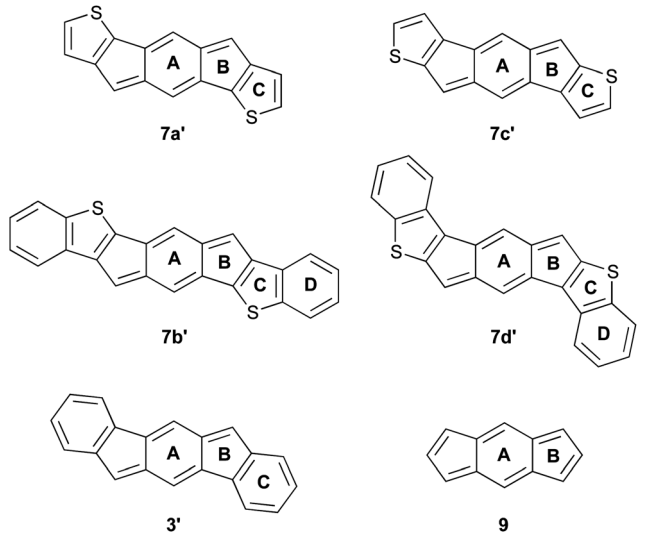


Fig. 4 Model IDTs/IDBTs **7a′–d′**, [1,2-*b*]IF **3′** and *s*-indacene **9** used for NICS(1) calculations.

with smaller HOMO-LUMO gaps than the [1,2-*b*]IFs. Tobe *et al.* very recently described unknown [2,1-*b*] isomer **6**;[10c] however, the instability of the molecule may preclude its use in organic electronics.

Given the analogy between pentacene and anthradithiophene, we were eager to build upon our previous successes and thus examine a similar structural analogy between the indeno [1,2-*b*]fluorene and indacenodithiophene skeletons. Herein we report the synthesis of two indacenedithiophenes (IDTs, **7a,c**) and two indacenedibenzothiophenes (IDBTs, **7b,d**) from the corresponding indacenedione precursors (**8a–d**, Fig. 3), along with the respective optical, electrochemical, computational, and structural data for this new class of electron-accepting molecules.

## Results and discussion

Our initial studies *in silico* of the simplified IDT structures **7a′–d′** (Fig. 4) suggested that the 20 π-electron, formally antiaromatic compounds should possess some interesting optical and electronic properties. NICS(1) calculations (Table 1) indicated that, compared to model [1,2-*b*]IF **3′**, the weaker aromaticity of the fused thiophenes (ring C in **7a′–d′**) would allow the antiaromaticity of the indacene core (rings A and B) to reassert itself to *ca.* 60–90% of that found for *s*-indacene (**9**). Calculations predicted lower low-energy transitions in the absorption spectrum, similar to what is observed with other strongly paratropic molecules.[12] The DFT calculations also predicted lower HOMO/LUMO energy levels and smaller energy gaps than for structurally analogous IFs. If these predictions hold true, then IDTs will differ significantly from ADTs, which show an *increase* in their gap energies compared to analogously derivatized pentacenes.[13]

The preparation of indacenedithiophenes **7a,c** and indacene-dibenzothiophenes **7b,d** followed the typical pathway to generate indenofluorenes—addition of a nucleophile to

Table 1 Calculated NICS(1)[a] values for rings A–D of IDTs **7a′–d′**, [1,2-*b*]IF **3′** and *s*-indacene **9**

| Entry | A | B | C | D |
|---|---|---|---|---|
| **3′** | 2.42 | 3.18 | −6.80 | na |
| **7a′** | 7.89 | 11.01 | −4.55 | na |
| **7b′** | 9.51 | 13.54 | −4.25 | −9.09 |
| **7c′** | 7.79 | 10.72 | −4.37 | na |
| **7d′** | 12.04 | 16.11 | −4.93 | −8.37 |
| **9** | 12.91 | 15.41 | na | na |

[a] DFT (B3LYP/6-311G**).

indacenediones **8a–d** followed by $SnCl_2$-mediated dearomatization. We elected to use mesityl lithium, anticipating based on the calculations that the bulky group would be needed to help kinetically stabilize the indacene core. Of the requisite diones, only **8a** is known;[14] diones **8b–d** were produced using a similar synthetic strategy, which is modified from the procedure used by McCulloch *et al.*[14a] Shown for **7d**/**8d** in Scheme 1, cross-coupling dibromide **10**[15] to stannane **11**[16] under Stille conditions generated diester **12**, which was subsequently saponified to diacid **13**. Conversion to the acid chloride followed by intramolecular Friedel–Crafts acylation furnished dione **8d**. Treatment with MesLi gave the crude diol, which in turn was reductively dearomatized with $SnCl_2$, affording fully conjugated **7d** (see ESI† for the preparation of all other compounds). A distinct advantage to this synthetic route is that the IDTs possess a defined structure, whereas ADT and its derivatives have typically been prepared and studied as an inseparable mixture of *syn*- and *anti*-isomers as a result of the regiorandom Aldol condensations used to generate the precursor dione molecules.[13,17]

IDTs **7a,c** and IDBTs **7b,d** were isolated as stable, dark blue-green solids in modest overall yields. As anticipated from the calculations, the $^1$H NMR spectra of **7a–d** corroborate the

Open Access Article. Published on 10 December 2013. Downloaded on 2/11/2026 1:50:36 PM.
This article is licensed under a Creative Commons Attribution 3.0 Unported Licence.

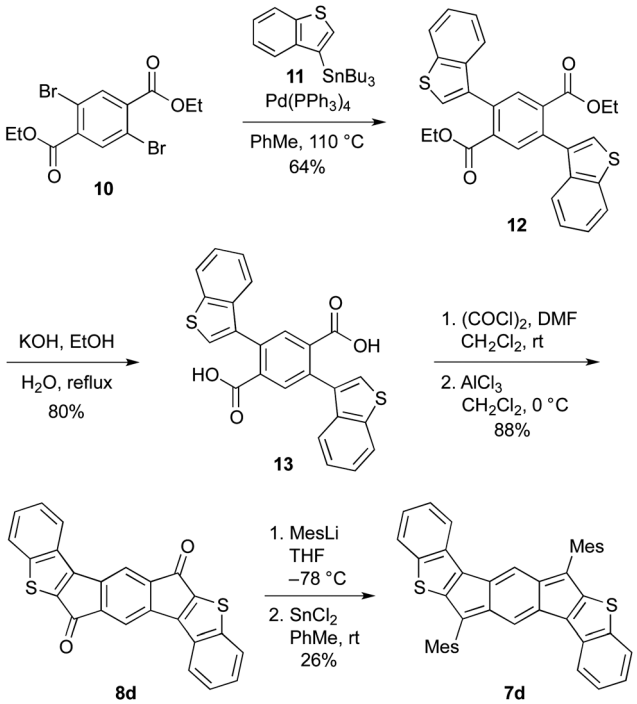


Scheme 1 Synthesis of IDBT **7d**.

stronger antiaromatic character of the IDTs: the signal for the protons on ring A appear at *ca.* 6.1 ppm, whereas the same protons in diones **8a–d** appear at about 7.3 ppm, and at about 7.1 ppm for the ring A protons in derivatives of **3** and **4**.

Fig. 5 and 6 show the electronic absorption spectra for diones **8** and IDTs **7**, respectively. These data along with calculated and experimental HOMO and LUMO energies and energy gaps are summarized in Table 2. The spectra of diones **8** display intense absorptions from approximately 275 nm to 325 nm with broad absorption bands attributable to weak $\pi \rightarrow \pi^*$ transitions appearing in the 550–600 nm range. The IDTs show maximum absorbance peaks ranging from 315 to 375 nm, but it is the lower energy absorptions that reveal clear differences

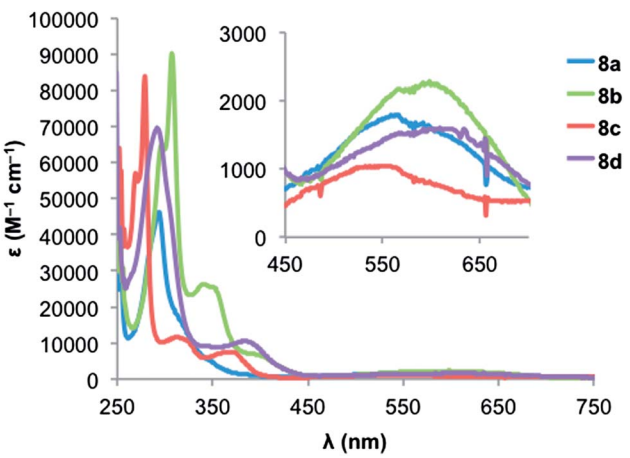


Fig. 5 Electronic absorption spectra of diones **8a–d** in DMSO.

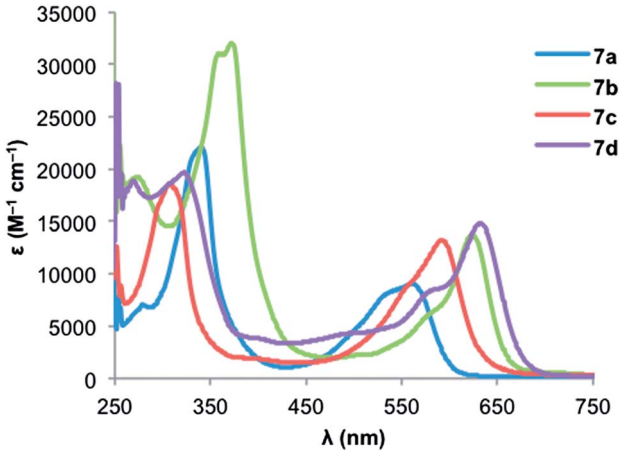


Fig. 6 Electronic absorption spectra of IDTs **7a–d** in DMSO.

between the thiophene-containing structures: (1) not surprisingly, the extended conjugation in IDBTs **7b,d** results in a lower $\lambda_{max}$ (624/632 nm) compared to the analogous IDTs **7a,c** (561/592 nm). (2) The "*syn*" isomers **7c,d** (S atom and Mes of adjacent rings on same side) possess a lower $\lambda_{max}$ compared to the analogous "*anti*" isomers **7a,b** (S atom and Mes of adjacent rings on opposite side). (3) As predicted by the calculations, the IDTs show a *decrease* in their gap energies by 0.2–0.3 eV compared to the analogous dimesityl derivative of indenofluorene **3b** (low energy $\lambda_{max}$ of 516 nm),[9c] which is in marked contrast to the aforementioned pentacene/ADT comparison.[13]

IDTs **7a,c** and IDBTs **7b,d** all undergo one reversible reduction in the solution state; however, the second reduction is essentially irreversible. The first oxidations of **7a** and **7c** were quasi-reversible and irreversible, respectively, whereas the first oxidations of **7b,d** were fully reversible under the experimental conditions (Fig 7). The extended π conjugation of the IDBTs had no significant effect on the HOMO energy levels compared to the IDTs; however, IDBTs possess LUMO levels 0.15–0.25 eV lower in energy than the corresponding IDTs. Calculated HOMO levels are in good agreement with those measured by cyclic voltammetry (Fig. 7 and 8), though calculated LUMO levels are higher than experimental levels, which is common for DFT derived LUMO levels of molecules featuring the *p*-quinodimethane motif.[9] Comparison of the HOMO and LUMO levels of similarly functionalized IFs shows that the HOMO is destabilized and the LUMO is stabilized by thiophene substitution compared to the all carbon analogues, resulting in a smaller bandgap as demonstrated by the longer wavelength $\lambda_{max}$. The presence of two reductions in IFs is typically attributed to the stabilization of the dianion by aromatization of the formally antiaromatic indacene core to give a $[4n + 2]$ π-electron system; similar behaviour was demonstrated for IDTs **7a,c** and IDBTs **7b,d**.

Diones **8a,c** were similarly assessed *via* CV, and each displayed two reversible reductions, with no accessible oxidations under the experimental conditions (Fig. 8). The poor solubility of the corresponding dibenzodiones **8b,d** in solvents amenable to electrochemical analysis precluded analogous investigation.


This journal is © The Royal Society of Chemistry 2014

Open Access Article. Published on 10 December 2013. Downloaded on 2/11/2026 1:50:36 PM.
This article is licensed under a Creative Commons Attribution 3.0 Unported Licence.

Table 2 Computational, electrochemical, and optical data for IDTs **7a–d** and diones **8a–d**

| | Computational[a] | | | Electrochemical[b] | | | | | | | Optical[c] |
|---|---|---|---|---|---|---|---|---|---|---|---|
| Compd | $E_{HOMO}$ | $E_{LUMO}$ | $E_{gap}$ | $E^1_{red}$ | $E^2_{red}$ | $E_{ox}$ | $E_{HOMO}$ | $E_{LUMO}$ | $E_{gap}$ | $\lambda_{max}$ | $E_{gap}$ |
| **7a** | −5.35 | −3.17 | 2.18 | −0.92 | −1.69[d] | 0.93 | −5.57 | −3.72 | 1.85 | 561 | 2.07 |
| **7b** | −5.30 | −3.34 | 1.96 | −0.80 | −1.62[d] | 0.92 | −5.56 | −3.84 | 1.72 | 624 | 1.88 |
| **7c** | −5.41 | −3.22 | 2.18 | −0.94 | −1.59[d] | 0.93[d] | −5.57[d] | −3.70 | 1.88 | 592 | 1.96 |
| **7d** | −5.29 | −3.46 | 1.84 | −0.61 | −1.24[d] | 0.98[d] | −5.62[d] | −4.03 | 1.59 | 632 | 1.83 |
| **8a**[e] | −6.12 | −3.40 | 2.72 | −0.91 | −1.49 | — | — | −3.73 | — | 566 | 1.75 |
| **8b**[f] | −5.99 | −3.47 | 2.51 | — | — | — | — | — | — | 598 | 1.66 |
| **8c**[e] | −6.22 | −3.41 | 2.81 | −0.87 | −1.27 | — | — | −3.77 | — | 551 | 1.89 |
| **8d**[f] | −5.94 | −3.51 | 2.43 | — | — | — | — | — | — | 609 | 1.56 |

[a] Calculations were performed at the B3LYP/6-31G** level of theory; energies are in eV. [b] CVs were recorded using 1–5 mM of analyte in 0.1 M $Bu_4NOTf/CH_2Cl_2$ at a scan rate of 50 mV $s^{-1}$ with a glassy carbon working electrode, a Pt coil counter electrode, and a Ag wire pseudo-reference. Values reported as the half-wave potential (*vs.* SCE) using the $Fc/Fc^+$ couple (0.46 V) as an internal standard. HOMO and LUMO energy levels in eV were approximated using SCE = −4.68 eV *vs.* vacuum (see ref. 18) and $E_{1/2}$ values for reversible processes or $E_p$ values for irreversible processes. [c] Spectra were obtained in DMSO; wavelengths are in nm. The optical HOMO/LUMO gap was determined as the intersection of the *x*-axis and a tangent line passing through the inflection point of the lowest-energy absorption; energies are in eV. [d] Reported as *V* at peak current, not half-wave potential. [e] Due to poor solubility in $CH_2Cl_2$ *o*-dichlorobenzene (ODCB) was used as solvent for electrochemical measurements. [f] Cyclic voltammetry measurements could not be obtained due to poor solubility of the compound.

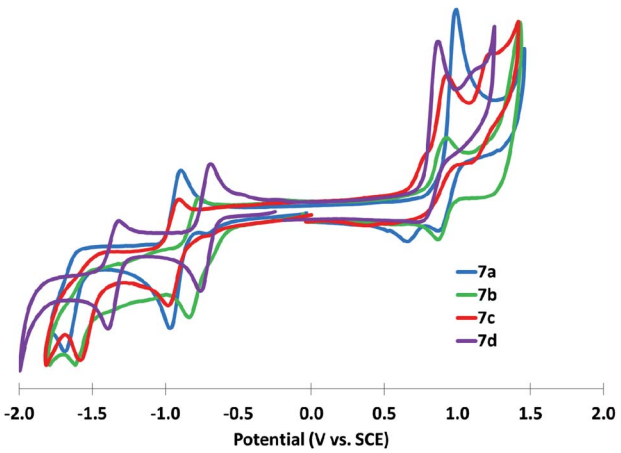


Fig. 7 Cyclic voltammetry of IDTs **7a–d**.

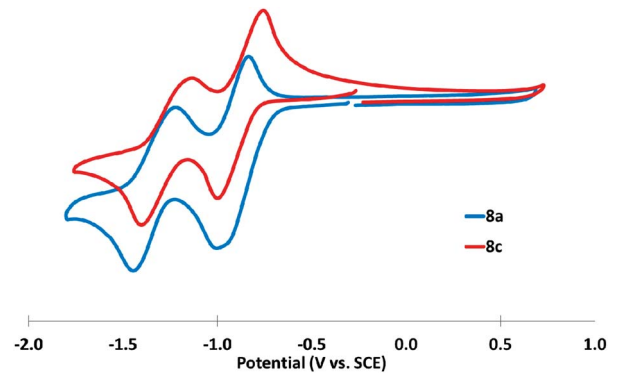


Fig. 8 Cyclic voltammetry of diones **8a** and **8c**.

Crystals suitable for X-ray diffraction were grown by diffusion of acetonitrile into $CH_2Cl_2$ (**7a,b,d**) or by slow evaporation of $CD_2Cl_2$ (**7c**). The structures of all four $C_2$-symmetric molecules are shown in Fig. 9; comparison of select bond lengths in the IDTs along with those in the dimesityl derivative of [1,2-*b*]IF **3b** are given in Table 3.[19] The lengths of the bonds in the central six-membered ring in **7a** and **3b** are quite similar ($\Delta$ 0.002–0.004 Å), while the bond lengths of the five-membered rings show more variability. This is not surprising given the five-membered rings are fused to thiophene rings in **7a**, and benzene rings in **3b**. Comparing **7a,c** to their benzo-fused counterparts **7b,d**, it can be seen that the bond lengths of the indacene core are more homogenous in **7b** and **7d**. This homogenization is indicative of increased paratropicity within this core in the benzo-fused IDTs, similar to what Hafner and co-workers observed for the 1,3,5,7-tetra-*tert*-butyl derivative of indacene **9**,[20] and is in agreement with NICS(1) values of rings **A** and **B** in Table 1. The dihedral angle between the average planes of the mesityl group and the IDT core is smaller for **7c** (63.6°) and **7d** (60.6°) than for **7a** (68.2°) and **7b** (74.3°), which presumably results in increased conjugation overall for the *syn* isomers compared to the *anti*. This could possibly explain the longer wavelength absorbances of the *syn* isomers compared to the *anti* isomers; otherwise, there are no significant structural differences between the *syn*/*anti* isomers.

Both **7a** and **7b** exhibit herringbone-like packing of the IDT core with the sulfur atoms participating in the closest intermolecular distances (Fig. 10). In the crystal structure of **7a**, each sulfur atom makes two short contacts with the five-membered ring of the adjacent molecules (3.312 and 3.421 Å) with a relatively long S···S contact (4.202 Å). While **7b** exhibits a similar crystal packing pattern, the extra benzo groups on this molecule force the sulfur atoms to be closest to the thiophene rings of the adjacent molecules; these S···C contacts are in the range 3.406–3.520 Å with the S···S contact of 3.707 Å.

The packing of **7d** is slightly different than **7a** and **7b** but also herringbone-like. The shortest C···C contacts between the central ring of one molecule and the peripheral ring of the other are 3.499 and 3.352 Å; unfortunately, the closest contact is at a

Open Access Article. Published on 10 December 2013. Downloaded on 2/11/2026 1:50:36 PM.
This article is licensed under a Creative Commons Attribution 3.0 Unported Licence.

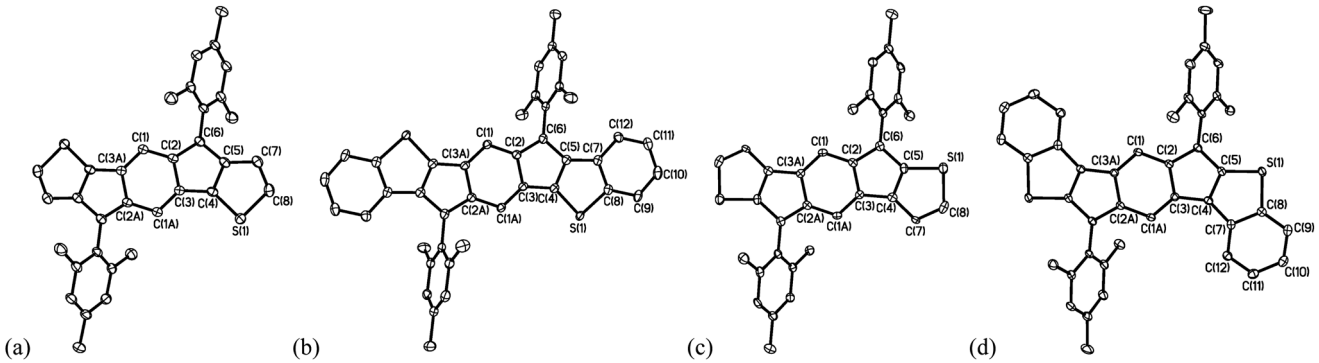


Fig. 9 Molecular structures of (a) **7a**, (b) **7b**, (c) **7c** and (d) **7d**; hydrogen atoms omitted for clarity. Ellipsoids drawn at 50% probability level.

Table 3 Select bond lengths (Å) of IDT **7a,c**, IDBTs **7b,d** and IF **3b**

| bond[a] | **7a** | **7b** | **7c** | **7d** | **3b** (R = Mes)[b] |
|---|---|---|---|---|---|
| C1–C2 | 1.431(2) | 1.412(3) | 1.418(3) | 1.421(2) | 1.433(3) |
| C1–C3A | 1.360(2) | 1.377(3) | 1.363(3) | 1.371(2) | 1.356(2) |
| C2–C3 | 1.469(2) | 1.457(3) | 1.456(3) | 1.454(2) | 1.467(2) |
| C2–C6 | 1.388(2) | 1.409(3) | 1.398(3) | 1.407(2) | 1.380(2) |
| C3–C4 | 1.452(2) | 1.437(3) | 1.461(3) | 1.457(2) | 1.469(3) |
| C4–C5 | 1.389(2) | 1.393(3) | 1.384(3) | 1.391(2) | 1.413(2) |
| C5–C6 | 1.460(2) | 1.435(3) | 1.447(3) | 1.441(2) | 1.471(2) |
| C5–C7 | 1.417(2) | 1.441(3) | 1.425(3)[c] | 1.429(2)[c] | na[e] |
| C7–C8 | 1.355(3) | 1.418(3) | 1.357(4) | 1.423(2) | na[e] |
| C4–S1 | 1.706(2) | 1.718(2) | 1.720(2)[d] | 1.730(2)[d] | na[e] |
| C8–S1 | 1.736(2) | 1.756(2) | 1.714(3) | 1.749(2) | na[e] |

[a] Numbering scheme shown in Fig. 9. [b] See ref. 9c. [c] C4–C7 in **7c,d**. [d] C5–S1 in **7c,d**. [e] Not applicable as the fused ring is benzene, not thiophene.

site with no significant LUMO density. IDT **7c** also exhibits a 1D structure with slight overlap of the thiophene units in neighbouring molecules, with a distance between the average planes of 3.615 Å; however, the parallel arrangement of the 1D columns relative to each other in the packing of **7c** is clearly different than the herringbone pattern in **7a**, **7b** and **7d** (Fig. 10). The shortest S···S contact in **7c** is 4.829 Å, showing that such interactions are not involved in directing the crystal packing.

## Conclusions

In summary, we have demonstrated the feasibility of fully conjugated indacenedithiophenes where both *syn* and *anti* isomers can be regioselectively synthesized. In tandem with computational findings, both optical and electrochemical data reveal stabilized HOMO and LUMO energy levels for **7a–d**. Unlike the anthradithiophene/pentacene analogy, indacenedithiophenes have smaller energy level gaps than their purely

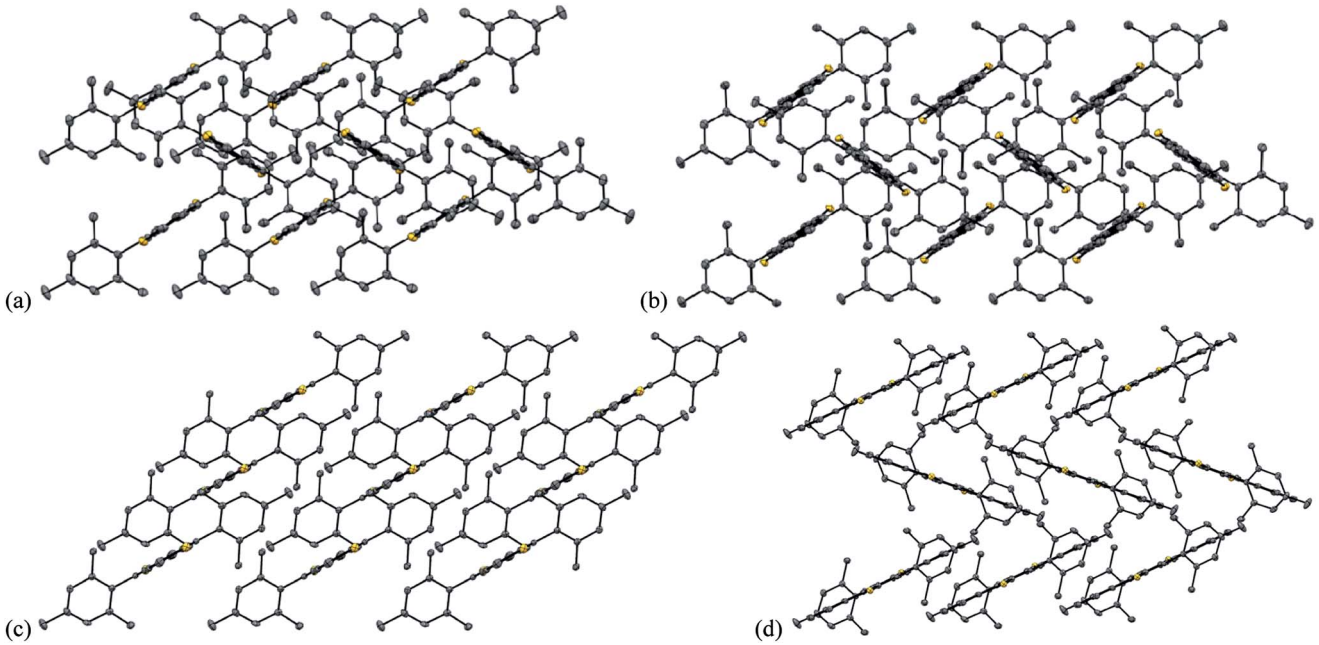


Fig. 10 Packing diagrams of (a) **7a**, (b) **7b**, (c) **7c** and (d) **7d**; hydrogen atoms omitted for clarity.


This journal is © The Royal Society of Chemistry 2014

Open Access Article. Published on 10 December 2013. Downloaded on 2/11/2026 1:50:36 PM. This article is licensed under a Creative Commons Attribution 3.0 Unported Licence.

hydrocarbon indenofluorene analogues, which is attributable to the increased paratropicity of the indacene core due to thiophene fusion. X-ray crystal packing reveals short intramolecular contact distances between LUMO-rich regions. Combined, these results suggest that **7a–d** could make excellent candidates for electronic applications. Future work will consist of exploring derivatization and oligomerization/polymerization of the IDT structure as well as device construction to test their performance as organic semiconductors.

## Acknowledgements

We thank the National Science Foundation (CHE-1013032 and CHE-1301485) for support of this research as well as support in the form of instrumentation (CHE-0923589) and computer grants (OCI-0960354). We also thank Prof. Mark Lonergan (University of Oregon) for use of his group's potentiostat. HRMS were obtained at the Mass Spectrometry Facilities and Services Core of the Environmental Health Sciences Center, Oregon State University, supported by grant #P30-ES00210, National Institute of Environmental Health Sciences, National Institutes of Health.

## Notes and references

1 (*a*) *Functional Organic Materials*, ed. T. J. J. Müller and U. H. F. Bunz, Wiley-VCH, Weinheim, Germany, 2007; (*b*) *Organic Light Emitting Devices: Synthesis, Properties and Applications*, ed. K. Mullen and U. Scherf, Wiley-VCH, Weinheim, Germany, 2006; (*c*) *Carbon-Rich Compounds*, ed. M. M. Haley and R. R. Tykwinski, Wiley-VCH, Weinheim, Germany, 2006; (*d*) F. M. Li, A. Nathan, Y. Wu and B. S. Ong, *Organic Thin Film Transistor Integration: A Hybrid Approach*, Wiley-VCH, Weinheim, Germany, 2011; (*e*) *Organic Electronics II*, ed. H. Klauk, Wiley-VCH, Weinheim, Germany, 2012.

2 (*a*) J. E. Anthony, *Chem. Rev.*, 2006, **106**, 5028–5048; (*b*) J. E. Anthony, *Angew. Chem., Int. Ed.*, 2008, **47**, 452–483.

3 (*a*) M. Bendikov, F. Wudl and D. F. Perepichka, *Chem. Rev.*, 2004, **104**, 4891–4945; (*b*) J. E. Anthony, A. Facchetti, M. Heeney, S. R. Marder and X. Zhan, *Adv. Mater.*, 2010, **22**, 3876–3892.

4 (*a*) J. Wu, W. Pisula and K. Müllen, *Chem. Rev.*, 2007, **107**, 718–747; (*b*) Z. Sun, Q. Ye, C. Chi and J. Wu, *Chem. Soc. Rev.*, 2012, **41**, 7857–7889.

5 (*a*) H. Usta, A. Facchetti and T. J. Marks, *J. Am. Chem. Soc.*, 2008, **130**, 8580–8581; (*b*) H. Usta, C. Risko, Z. Wang, H. Huang, M. K. Deliomergolu, A. Zhukhovitskiy, A. Facchetti and T. J. Marks, *J. Am. Chem. Soc.*, 2009, **131**, 5586–5608.

6 (*a*) Z. U. Levi and T. D. Tilley, *J. Am. Chem. Soc.*, 2009, **131**, 2796–2797; (*b*) T. Kawase, A. Konishi, Y. Hirao, K. Matsumoto, H. Kurata and T. Kubo, *Chem.–Eur. J.*, 2009, **15**, 2653–2661; (*c*) A. R. Mohebbi and F. Wudl, *Chem.–Eur. J.*, 2011, **17**, 2642–2646; (*d*) A. R. Mohebbi, J. Yuen, J. Fan, C. Munoz, M. F. Wang, R. S. Shirazi, J. Seifter and F. Wudl, *Adv. Mater.*, 2011, **23**, 4644–4648; (*e*) C. Lütke-Eversloh, Y. Avlasevich, C. Li and K. Müllen, *Chem.–Eur. J.*, 2011, **17**, 12756–12762; (*f*) J. D. Wood, J. L. Jellison, A. D. Finke, L. Wang and K. N. Plunkett, *J. Am. Chem. Soc.*, 2012, **134**, 15783–15789.

7 (*a*) J. G. Laquindandum, H. E. Katz and A. J. Lovinger, *J. Am. Chem. Soc.*, 1998, **120**, 664–672; (*b*) K. Takimiya, S. Shinamura, I. Osaka and E. Miyazaki, *Adv. Mater.*, 2011, **23**, 4347–4370.

8 (*a*) I. Kaur, W. Jia, R. P. Kopreski, S. Selvarasah, M. R. Dokmeci, C. Pramanik, N. E. McGruer and G. P. Miller, *J. Am. Chem. Soc.*, 2008, **130**, 16274–16286; (*b*) B. H. Northrop, K. N. Houk and A. Maliakal, *Photochem. Photobiol. Sci.*, 2008, **7**, 1463–1468; (*c*) Y. Li, Y. Wu, P. Liu, Z. Prostran, S. Gardner and B. S. Ong, *Chem. Mater.*, 2007, **19**, 418–423; (*d*) A. Maliakal, K. Raghavachari, H. Katz, E. Chandross and T. Siegrist, *Chem. Mater.*, 2004, **16**, 4980–4986; (*e*) K. Ono, H. Totani, T. Hiei, A. Yoshino, K. Saito, K. Eguchi, M. Tomura, J.-I. Nishida and Y. Yamashita, *Tetrahedron*, 2007, **63**, 9699–9704.

9 (*a*) D. T. Chase, B. D. Rose, S. P. McClintock, L. N. Zakharov and M. M. Haley, *Angew. Chem., Int. Ed.*, 2011, **50**, 1127–1130; (*b*) D. T. Chase, A. G. Fix, B. D. Rose, C. D. Weber, S. Nobusue, C. E. Stockwell, L. N. Zakharov, M. C. Lonergan and M. M. Haley, *Angew. Chem., Int. Ed.*, 2011, **50**, 11103–11106; (*c*) D. T. Chase, A. G. Fix, S. J. Kang, B. D. Rose, C. D. Weber, Y. Zhong, L. N. Zakharov, M. C. Lonergan, C. Nuckolls and M. M. Haley, *J. Am. Chem. Soc.*, 2012, **134**, 10349–10352; (*d*) A. G. Fix, P. E. Deal, C. L. Vonnegut, B. D. Rose, L. N. Zakharov and M. M. Haley, *Org. Lett.*, 2013, **15**, 1362–1365.

10 (*a*) A. Shimizu and Y. Tobe, *Angew. Chem., Int. Ed.*, 2011, **50**, 6906–6910; (*b*) J. Nishida, S. Tsukaguchi and Y. Yamashita, *Chem.–Eur. J.*, 2012, **18**, 8964–8970; (*c*) A. Shimizu, R. Kishi, M. Nakano, D. Shiomi, K. Sato, T. Takui, I. Hisaki, M. Miyata and Y. Tobe, *Angew. Chem., Int. Ed.*, 2013, **52**, 6076–6079; (*d*) H. Miyoshi, S. Nobusue, A. Shimizu, I. Hisaki, M. Miyata and Y. Tobe, *Chem. Sci.*, 2014, **5**, 163–168; (*e*) See also: D. K. Frantz, J. J. Walish and T. M. Swager, *Org. Lett.*, 2013, **15**, 4782–4785.

11 A. G. Fix, D. T. Chase and M. M. Haley, in *Topics in Current Chemistry*, ed. J. S. Siegel and Y.-T. Wu, Springer, Berlin, Germany, DOI: 10.1007/128_2012_376, in press.

12 (*a*) P. J. Garratt, *Aromaticity*, Wiley-Interscience, New York, NY, 1986; (*b*) H. Hopf, *Classics in Hydrocarbon Chemistry*, Wiley-VCH, Weinheim, Germany, 2000.

13 (*a*) M. M. Payne, S. A. Odom, S. R. Parkin and J. E. Anthony, *Org. Lett.*, 2004, **6**, 3325–3328; (*b*) M. M. Payne, S. R. Parkin, J. E. Anthony, C.-C. Kuo and T. N. Jackson, *J. Am. Chem. Soc.*, 2005, **127**, 4986–4987; (*c*) S. Subramanian, S. K. Park, S. R. Parkin, V. Podzorov, T. N. Jackson and J. E. Anthony, *J. Am. Chem. Soc.*, 2008, **130**, 2706–2707.

14 (*a*) W. Zhang, J. Smith, S. E. Watkins, R. Gysel, M. McGehee, A. Salleo, J. Kirkpatrick, S. Ashraf, T. Anthopoulos, M. Heeney and I. McCulloch, *J. Am. Chem. Soc.*, 2010, **132**, 11437–11439; (*b*) X. Wang, H. Luo, Y. Sun, M. Zhang, X. Li, G. Yu, Y. Liu, Y. Li and H. Wang, *J. Polym. Sci., Part A: Polym. Chem.*, 2012, **50**, 371–377.

Open Access Article. Published on 10 December 2013. Downloaded on 2/11/2026 1:50:36 PM. This article is licensed under a Creative Commons Attribution 3.0 Unported Licence.

15 K.-T. Wong, T.-C. Chao, L.-C. Chi, Y.-Y. Chu, A. Balaiah, S.-F. Chiu, Y.-H. Liu and Y. Wang, *Org. Lett.*, 2006, **8**, 5033–5036.

16 D. D. Dixon, M. A. Tius, G. A. Thakur, H. Zhou, A. L. Bowman, V. G. Shukla, Y. Peng and A. Makriyannis, *Bioorg. Med. Chem. Lett.*, 2012, **22**, 5322–5325.

17 Isomerically pure ADT derivatives have been prepared very recently, but their synthesis/separation tends to be considerabley more involved. While attempting to answer the long-standing question of whether or not isomerically pure materials would afford better device performance than those based on an isomeric mixture, the answer is still subject to debate, as some studies conclude there is no difference in device performance (a) whereas others note a marked difference with isomerically pure material (b and c). See: (*a*) D. Lehnherr, A. R. Waterloo, K. P. Goetz, M. M. Payne, F. Hampel, J. E. Anthony, O. D. Jurchescu and R. R. Tykwinski, *Org. Lett.*, 2012, **14**, 3660–3663; (*b*) Z. Li, Y.-F. Lim, J. B. Kim, S. R. Parkin, Y.-L. Loo, G. G. Malliaras and J. E. Anthony, *Chem. Commun.*, 2011, **47**, 7617–7619; (*c*) S. Mamada, T. Minamiki, H. Katagiri and S. Tokito, *Org. Lett.*, 2012, **14**, 4062–4065.

18 H. Reiss and A. Heller, *J. Phys. Chem.*, 1985, **89**, 4207–4213.

19 Crystallographic data for **7a**: $C_{34}H_{28}S_2$, $M_r = 500.68$, crystal size 0.17 × 0.14 × 0.03 $mm^3$, monoclinic, space group $P2_1/c$, $a = 14.2992(6)$, $b = 7.0840(3)$, $c = 13.4824(6)$ Å, $\beta = 108.840(2)^\circ$, $V = 1292.5(1)$ $Å^3$, $Z = 2$, $Z' = 0.5$, $\rho_{calc.} = 1.286$ g $cm^{-3}$, $\mu = 2.014$ $mm^{-1}$, $F(000) = 528$, CuK$\alpha$ radiation $\lambda = 1.54178$ Å, $T = 100(2)$ K, $2\Theta_{max} = 135.64^\circ$, 9736 reflections measured [$R_{int} = 0.0680$], 2315 reflections observed, 219 refined parameters, $R1 = 0.0398$, $wR2 = 0.1170$, and GOF = 1.083 for reflections with $I > 2\sigma(I)$, $R1 = 0.0418$, $wR2 = 0.1194$, and GOF = 1.083 for all data, max/min residual electron density +0.391/−0.328 e $Å^{-3}$. CCDC 949864. Crystallographic data for **7b**: $C_{42}H_{32}S_2$, $M_r = 600.80$, crystal size 0.19 × 0.10 × 0.02 $mm^3$, monoclinic, space group $P2_1/n$, $a = 13.689(2)$, $b = 7.3177(12)$, $c = 17.167(3)$ Å, $\beta = 112.808(3)^\circ$, $V = 1585.2(4)$ $Å^3$, $Z = 2$, $Z' = 0.5$, $\rho_{calc.} = 1.259$ g $cm^{-3}$, $\mu = 0.198$ $mm^{-1}$, $F(000) = 632$, MoK$\alpha$ radiation $\lambda = 0.71073$ Å, $T = 100(2)$ K, $2\Theta_{max} = 54.00^\circ$, 10 867 reflections measured [$R_{int} = 0.0518$], 3372 reflections observed, 263 refined parameters, $R1 = 0.0483$, $wR2 = 0.1135$, and GOF = 1.047 for reflections with $I > 2\sigma(I)$, $R1 = 0.0730$, $wR2 = 0.1261$, and GOF = 1.047 for all data, max/min residual electron density +0.485/−0.265 e $Å^{-3}$. CCDC 949866. Crystallographic data for **7c**: $C_{17}H_{14}S_2$, $M_r = 250.34$, crystal size 0.14 × 0.04 × 0.02 $mm^3$, triclinic, $P\bar{1}$, $a = 7.9092(14)$, $b = 8.0857(14)$, $c = 10.8326(19)$ Å, $\alpha = 91.725(4)^\circ$, $\beta = 107.227(4)^\circ$, $\gamma = 105.087(4)^\circ$, $V = 634.54(19)$ $Å^3$, $Z = 2$, $Z' = 0.5$, $\rho_{calc.} = 1.310$ g $cm^{-3}$, $\mu = 0.234$ $mm^{-1}$, $F(000) = 264$, MoK$\alpha$ radiation $\lambda = 0.71073$ Å, $T = 100(2)$ K, $2\Theta_{max} = 50^\circ$, 8463 reflections measured [$R_{int} = 0.0304$], 2237 reflections observed, 219 refined parameters, $R1 = 0.0449$, $wR2 = 0.1126$, and GOF = 1.005 for reflections with $I > 2\sigma(I)$, $R1 = 0.0549$, $wR2 = 0.1196$, and GOF = 1.005 for all data, max/min residual electron density +0.601/−0.366 e $Å^{-3}$. CCDC 962726. Crystallographic data for **7d**: $C_{42}H_{32}S_2$, $M_r = 600.80$, crystal size 0.20 × 0.17 × 0.09 $mm^3$, monoclinic, $P2_1/c$, $a = 14.4327(5)$, $b = 11.8497(4)$, $c = 8.9975(3)$ Å, $\beta = 94.020(1)^\circ$, $V = 1534.99(9)$ $Å^3$, $Z = 2$, $Z' = 0.5$, $\rho_{calc.} = 1.300$ $gcm^{-3}$, $\mu = 0.204$ $mm^{-1}$, $F(000) = 632$, MoK$\alpha$ radiation $\lambda = 0.71073$ Å, $T = 100(2)$ K, $2\Theta_{max} = 55.98^\circ$, 15512 reflections measured [$R_{int} = 0.0358$], 3659 reflections observed, 199 refined parameters, $R1 = 0.0472$, $wR2 = 0.1298$, and GOF = 1.039 for reflections with $I > 2\sigma(I)$, $R1 = 0.529$, $wR2 = 0.1350$, and GOF = 1.039 for all data, max/min residual electron density +0.568/−0.568 e $Å^{-3}$. CCDC 949865. These data can be obtained free of charge from The Cambridge Crystallographic Data Centre via www.ccdc.cam.ac.uk/data_request/cif.

20 (*a*) K. Hafner, B. Stowasser, H.-P. Krimmer, S. Fischer, M. C. Böhm and H. J. Lindner, *Angew. Chem., Int. Ed. Engl.*, 1986, **25**, 630–632; (*b*) See also: J. D. Dunitz, C. Krüger, H. Irngartinger, E. F. Maverick, Y. Wang and M. Nixdorf, *Angew. Chem., Int. Ed. Engl.*, 1988, **27**, 387–389.

 This journal is © The Royal Society of Chemistry 2014